

A Theoretical Insight into the Interaction of Fatty Acids Involved in Royal Jelly with the Human Estrogen Receptor β

Toshiaki Matsubara,*[1] Hiroyuki Sugimoto,[2] and Misako Aida[1]

[1]Center for Quantum Life Sciences and Graduate School of Science, Hiroshima University, 1-3-1, Kagamiyama, Higashi-Hiroshima 739-8530

[2]Yamada Apiculture Center, Inc., 194, Ichiba, Kagamino, Tomata, Okayama 708-0393

Received April 22, 2008; E-mail: matsu05@hiroshima-u.ac.jp

It has been well-known that fatty acids occurring in the royal jelly of honeybees are effective towards autonomic imbalance, perimenopausal symptoms, osteoporosis, and other conditions. These pharmacological effects of royal jelly similar to those caused by the hormone estrogen are thought to appear due to the interaction of the fatty acids of royal jelly with an estrogen receptor inside the human body. Although the structure of several major fatty acids present in royal jelly has been determined experimentally, no direct evidence of the interaction of these fatty acids with the estrogen receptor have been reported yet. In this study, we therefore give an insight into the interaction of fatty acids with the human estrogen receptor β by quantum mechanical (QM), ONIOM, and molecular dynamics (MD) methods using a model active site.

Royal jelly, which is secreted from the hypopharyngeal glands in the heads of young worker honeybees (*Apis mellifera*),[1,2] is the principal food for the larvae of the queen honeybee. All of the female larvae in a colony, including those destined to become workers, are for their growth fed royal jelly for the first three days after hatching. After the first three days, only the queen continues to be fed royal jelly. This feeding triggers the development of queen morphology, including the fully developed ovaries needed to lay eggs. It is very surprising that the life span of the queen is 2–5 years compared to the considerably short life span of workers, 2–3 months or less. The nutritional significance of royal jelly is the fact that the differentiation of the female larvae is determined by the nature of their diet in their early development stage.[3] This extraordinary nature of royal jelly has stirred many researchers to study its chemical nature and pharmacological actions.

Royal jelly is now used worldwide in commercial medical products, health foods, and cosmetics, due to its life-extending,[4] antifatigue,[5] antiallergic,[6] antitumor,[7] antihypercholesterolemic,[8] antihypertensive,[9] anti-inflammatory,[10] and other effects. Royal jelly is a creamy, yellow-white, and acidic substance, and its chemical composition is water, crude protein, simple sugars, and fatty acids. It also contains a trace amount of minerals, some enzymes, antibacterial and antibiotic components, and vitamins. Bioactive substances such as fatty acids,[11] proteins,[5,6] and antibacterial protein[12] contained in royal jelly are thought to be beneficial towards treatment of osteoporosis and menopausal symptoms.

Several saturated and unsaturated fatty acids present in royal jelly have been isolated and their structures have been determined. Fatty acids of royal jelly are chemically unique and unlike those of most animal and plant materials. They have short chains with 8–10 carbons, and most of them are hydroxy fatty acids or dicarboxylic acid. The main fatty acids detected from royal jelly experimentally are as follows; (*E*)-10-hydroxy-2-decenoic acid, 8-hydroxyoctanoic acid, 10-hydroxydecanoic acid, (*E*)-2-decenedioic acid, (*E*)-9-hydroxy-2-decenoic acid, and (3*R*)-3,10-dihydroxydecenoic acid.[13] (*E*)-10-hydroxy-2-decenoic acid, which has not been found in other natural product so far, has been reported to have some pharmacological activities.[14–16] It is also known that the queen-produced (*E*)-9-hydroxy-2-decenoic acid has a swarm-stabilizing activity.[17]

The pharmacological effects of the fatty acids of royal jelly on autonomic imbalance, perimenopausal symptoms, and osteoporosis, similar to those caused by the hormone estrogen, are thought to appear when fatty acids of royal jelly interact with the estrogen receptor inside the human body. In fact, it has been reported that (*E*)-10-hydroxy-2-decenoic acid and 10-hydroxydecanoic acid exhibit activity for estrogen receptor β.[18] However, there is no direct evidence of interaction of fatty acids with estrogen receptors. No crystal structure of a fatty acid of royal jelly binding with the estrogen receptor has been reported yet. Therefore, we focus on the crystal structure of genistein that binds with the human estrogen receptor β, because genistein, which is known as a soybean isoflavone, acts on osteoporosis as an agonist like fatty acids.[19,20]

In this study, we examined whether the fatty acids fit the pocket and interact with the active site of the human estrogen receptor β for genistein, using quantum mechanical and ONIOM methods. We adopted a set of saturated and unsaturated hydroxy fatty acids to examine a tendency in the binding energy. We used two kinds of model of the active site, models A and B, constructed from the crystal structure for genistein to examine the environmental effects on the binding of the ligands. The molecular dynamics simulations are also performed to give further insight into the interaction of the ligands inside the pocket taking account of thermal motion.

Published on the web October 10, 2008; doi:10.1246/bcsj.81.1258

Computational Details

Selected Fatty Acids Involved in Royal Jelly as Ligands. Although not all the fatty acids occurring in royal jelly have been clarified yet, the dominant fatty acids have been isolated as mentioned in the Introduction. The unsaturated hydroxy fatty acid, (*E*)-10-hydroxy-2-decenoic acid and (*E*)-9-hydroxy-2-decenoic acid, and the saturated hydroxy fatty acid, 10-hydroxydecanoic acid and 8-hydroxyoctanoic acid, are mainly included in royal jelly. On the basis of this fact, we adopted a set of unsaturated hydroxy fatty acids with the –OH group in different positions and of saturated hydroxy fatty acids with different chain length as follows to examine the trend in the binding strength at the active site of the estrogen receptor; unsaturated fatty acids: (*E*)-10-hydroxy-2-decenoic acid (10H2DA), (*E*)-9-hydroxy-2-decenoic acid (9H2DA), (*E*)-8-hydroxy-2-decenoic acid (8H2DA), (*E*)-7-hydroxy-2-decenoic acid (7H2DA); saturated fatty acids: 10-hydroxydecanoic acid (10HDA), 9-hydroxynonanoic acid (9HNA), 8-hydroxyoctanoic acid (8HOA). Their skeletal formulas are depicted in Scheme 1. Of these fatty hydroxy acids, 8H2DA, 7H2DA, and 9HNA have not been detected experimentally so far from royal jelly. In addition to these hydroxy fatty acids, we adopted two artificial unsaturated fatty acids, (*E*)-10,10-dihydroxy-2-decenoic acid (10,10H2DA) and (*E*)-9,10,10-trihydroxy-2-decenoic acid (9,10,10H2DA) to examine the effect of an additional –OH group on the binding. The abbreviations in parentheses are used below as the name of the ligand. GEN is used for genistein.

Models of the Active Site. We selected the crystal structure of the estrogen receptor β that binds with the ligand genistein, which is registered in the protein data bank (PDB) with the ID code 1QKM,[21] to construct a model pocket of the active site. It is well-known that three amino acid residues, Glu, Arg, His, and bound water play an important role in the binding of ligands through H-bonds in the active site. We therefore cut out these three key amino acid residues and bound water from the crystal structure of 1QKM and constructed simple model A as presented in Figure 1. In order to consider the environmental effects on the binding of the ligand, we constructed more sophisticated model B presented in Figure 1. Model B includes the additional ten amino acid residues, Leu301, Leu298, Met296, Leu476, Ile373, Ile376, Gly472, Met340, Met336, Leu339, which are essential amino acid residues to make the shape of the pocket of the active site and considered to significantly affect the ligand sterically and electrostatically.

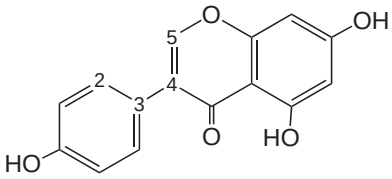

Genistein

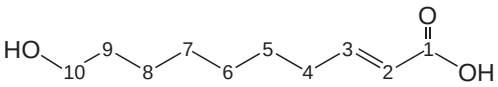

Unsaturated hydroxy fatty acid

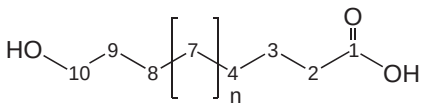

n=1,2,3

Saturated hydroxy fatty acid

Scheme 1.

Calculation Methods. All the quantum mechanical (QM) calculations were performed using the Gaussian03 program.[22] For model A, the geometry optimizations were performed at the Hartree–Fock (HF) level of theory with the 6-31G* basis set for all the atoms. We confirmed that the conformation of 10H2DA is well reproduced at this level as

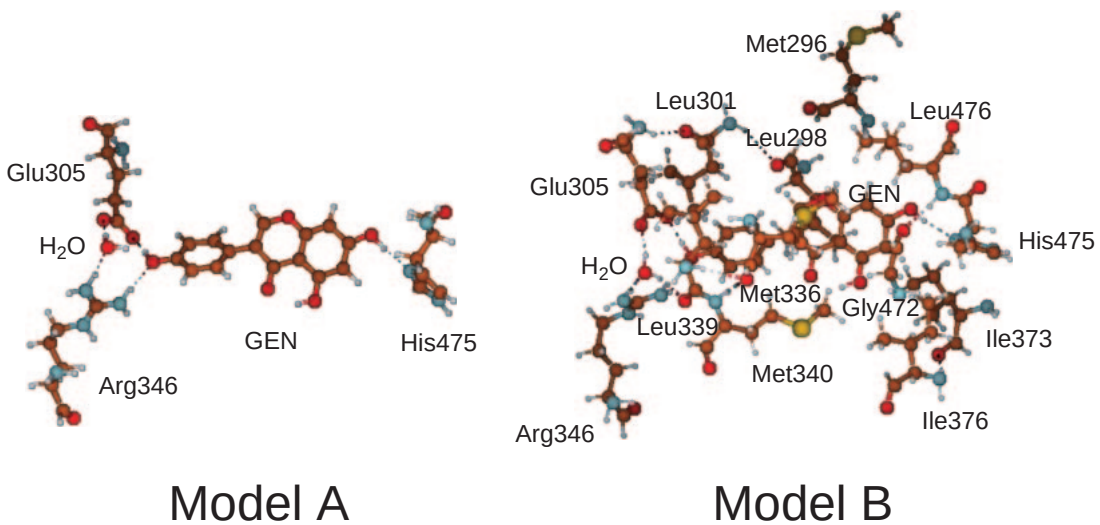

Figure 1. Models A and B of the active site of the human estrogen receptor β with the ligand genistein. Model A includes three essential amino acid residues, Glu305, Arg346, and His 475, and the bound water with which genistein forms H-bonds in the crystal structure. Model B includes an additional ten amino acid residues, Leu301, Leu298, Met296, Leu476, Ile373, Ile376, Gly472, Met340, Met336, Leu339, which make the pocket and have steric and electrostatic interactions with genistein.

mentioned in the next section. In the geometry optimizations, the position of the α-carbon of all the amino acid residues, four atoms attached to their α-carbon, and the oxygen of the bound water were fixed to keep the features of the pocket of the active site of the crystal structure. The energies were improved with more reliable basis set 6-31G** taking account of the electron correlation at the B3LYP level of the density function theory (DFT) method. The basis set super position error (BSSE) in the interaction of the ligand with the amino acid residues was corrected by the counterpoise method.[23,24]

We used the ONIOM method[25–31] for the geometry optimizations and the energy calculations for model B, where the entire system was divided into two layers. The inner part, which includes the ligand and three amino acid residues, Glu305, Arg346, and His475, and the bound water, corresponds to model A. The outer part includes the other ten amino acid residues, Leu301, Leu298, Met296, Leu476, Ile373, Ile376, Gly472, Met340, Met336, and Leu339. The geometry optimizations were performed at the ONIOM(HF/6-31G*:PM3) level fixing the position of the α-carbon of all the amino acid residues, four atoms attached to their α-carbon, and the oxygen of the bound water to keep the shape of the pocket of the active site of the crystal structure. The energies were improved at the ONIOM(HF/6-31G**:PM3) and ONIOM(B3LYP/6-31G**:PM3) levels and the basis set super position error (BSSE) in the interaction of the ligand with the amino acid residues in the inner part was removed by the counterpoise method. All the optimized structures for models A and B are presented as Supporting Information.

The molecular dynamics (MD) simulations were performed using the TINKER program[32] with the MM3 force filed parameters.[33–37] The motion of the nuclei was evolved by the Beeman algorithm[38] Here, the position of the α-carbon of all the amino acid residues, four atoms attached to their α-carbon, and the oxygen of the bound water were fixed similarly to keep the shape of the pocket of the active site of the crystal structure. The simulations were run under a constant temperature of 300 K through the use of Berendsen's velocity scaling algorithm[39] with a time step of 1 fs for 100 ps. The average and standard deviation of the geometric parameters and the probability of the interaction were calculated from the data collected every 10 fs.

Conformation of (*E*)-10-Hydroxy-2-decenoic Acid. Although the saturated fatty acids form straight chains, the unsaturated fatty acids with a double bond, such as (*E*)-10-hydroxy-2-decenoic acid, do not (see picture below). This is reasonably understood by the fact that 1-butene does not take trans conformation.[40,41] We calculated the conformation energy of 1-butene ourselves at the various levels and compared it to that of (*E*)-10-hydroxy-2-decenoic acid (Chart 1).

We calculated the conformation energy surface of 1-butene varying the levels from HF/3-21G to MP2/6-31G**. As presented in Figure 2, no level changes the tendency in the energy

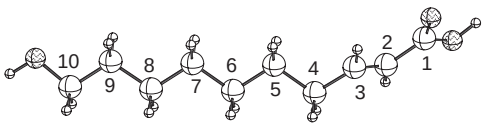

Chart 1.

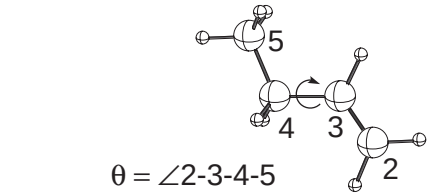

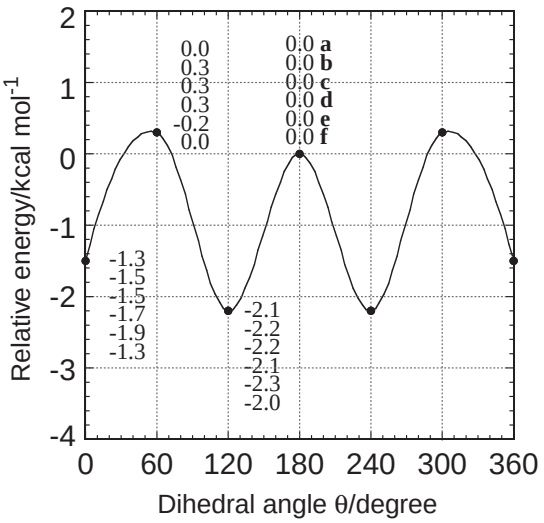

Figure 2. Energy changes of 1-butene and (*E*)-10-hydroxy-2-decenoic acid by the dihedral angle θ at the various levels. 1-Butene; a: HF/3-21G, b: HF/6-31G*, c: HF/6-31G**, d: B3LYP/6-31G**, e: MP2/6-31G**, and (*E*)-10-hydroxy-2-decenoic acid; f: HF/6-31G*.

Table 1. Optimized Dihedral Angle θ at the Various Levels for the Most Stable Equilibrium Structures of 1-Butene and (*E*)-10-Hydroxy-2-decenoic Acid

Level	Dihedral angle θ[a)]
1-Butene	
HF/3-21G	116.7
HF/6-31G*	119.7
HF/6-31G**	119.8
B3LYP/6-31G**	119.7
MP2/6-31G**	117.7
(*E*)-10-Hydroxy-2-decenoic acid	
HF/6-31G*	120.3
MM3	113.8

a) For dihedral angle θ, see Figure 2.

surface. Two minima exist at the dihedral angle θ of around 0 and 120°. The energy reaches the maximum at the dihedral angle θ of around 60 and 180°. When θ is about 120°, the structure is the most stable in energy at any level. Although we calculated the energy surface at the higher levels, CCSD(T), QCISD(T), MP4SDQ with the basis set 6-311++G**, these tendencies did not change at all. These relative energies of the conformation of 1-butene are consistent with previous computational results.[40,41]

A list of the values of the dihedral angle θ of the most stable equilibrium structure is presented in Table 1. For 1-butene, θ

Table 2. Distances of the H-Bonds of the Various Ligands with the Surrounding Amino Acid Residues and Bound Water and the Selected Dihedral Angles of the Ligands in the Optimized Structures of Model A at the HF/6-31G* Level

Ligand	Distance of the H-bonds/Å				Dihedral angle/degree[a)]	
	Glu305	Arg346	Bound water	His475	∠2–3–4–5	∠10–9–8–7
GEN	1.610	1.924	2.291	1.932	49.0 (49.1)	
10H2DA	1.708	1.770		2.001	−130.3 (−120.3)	−168.7 (−180.0)
9H2DA	1.969			1.962	−124.9 (−120.3)	−170.1 (−175.8)
8H2DA	1.898		2.125	2.039	−128.0 (−120.4)	−170.9 (−176.3)
7H2DA				1.969	−0.6 (−120.2)	−177.3 (−176.9)
10HDA	1.723	1.755		1.944	177.8 (180.0)	−167.8 (178.8)
9HNA	1.657	1.860	2.049	1.940	177.3 (179.9)	−179.3 (180.0)
8HOA	2.005			1.978	−179.8 (179.8)	−178.4 (179.7)
10,10H2DA	1.709	1.818	1.900	2.001	−128.7 (−120.3)	−167.6 (179.8)
9,10,10H2DA	1.781/1.885	1.858/2.299/2.502	2.049	1.935	119.9 (−120.3)	−155.5 (−175.1)

a) The values in the parentheses are for the optimized structures of the fee ligands.

is about 117–120°. (*E*)-10-Hydroxy-2-decenoic acid also gives a similar value of 120.3° at the HF/6-31G* level. We confirmed that the MM3 force field used for MD simulations gives a similar θ of 113.8° for (*E*)-10-hydroxy-2-decenoic acid.

Results and Discussion

QM Calculations for Model A. In this section, we first discuss model A without the amino acid residue environment to clarify the environmental effects, comparing with model B with the amino acid residue environment in the next section. The optimized structure for GEN is presented in Figure S3. One of the –OH groups interacts with Arg346 and the bound water in addition to Glu305 through a H-bond. The H-bond with Glu305 has the shortest distance of 1.610 Å as presented in Table 2. Hereafter, if the bond length is less than 3 Å, we recognize its bond as a H-bond. The other –OH group forms a H-bond with His475 with a distance of 1.932 Å. The dihedral angle ∠2–3–4–5 of 49.0° is nearly the same as that of 49.1° for the free GEN.

The unsaturated hydroxy fatty acid, 10H2DA, also interacts with Glu305, Aeg346, and His475 by three H-bonds, although the –OH oxygen is a little far from a bound water hydrogen to form a H-bond. By these interactions, the main chain of 10H2DA is deformed, as shown by two dihedral angles, ∠2–3–4–5 and ∠10–9–8–7, which change by about 10° compared to those of the free 10H2DA. On the other hand, 9H2DA forms H-bonds only with Glu305 and His475, and the –OH group is not allowed to form a H-bond with Arg346, because the –OH group is shifted to the C-9 position. However, the –OH group at the C-8 position in 8H2DA, which is located in the vicinity of the bound water, forms a H-bond with the bound water beside Glu305 (See Figure S1). For 7H2DA, the –OH group at the C-7 position is located completely separated from Glu305, His475, and bound water. Therefore, only a –COOH group forms a H-bond with His475. The main chain forms another conformation with the dihedral angle ∠2–3–4–5 of 0.6° to keep the alkyl group away from Glu305 and reduce the steric repulsion between them.

The saturated hydroxy fatty acid, 10HDA, interacts with Glu305, Arg346, and His475 by three H-bonds, which is similar to the case of the unsaturated hydroxy fatty acid 10H2DA. However, the deformation in the terminal region becomes large as shown by the small dihedral angle ∠10–9–8–7 of −167.8°, since the carbon chain taking a straight form requires a larger space. The shorter 9HNA reduces this deformation and forms an additional H-bond between the –OH group and the bound water. On the other hand, 8HOA is too short to form H-bonds of the –OH group with Arg346 and the bound water.

The unsaturated hydroxy fatty acid 10,10H2DA that has the second –OH group at the C-10 position forms additional H-bonds with the bound water. 9,10,10H2DA with the second and third –OH groups at the C-9 and C-10 position further forms some new H-bonds with Glu305 and Arg346. However, one will notice that the additional H-bonds increase the deformation of the terminal region of the carbon chain as shown by the smaller dihedral angles of ∠2–3–4–5 and ∠10–9–8–7 in both cases of 10,10H2DA and 9,10,10H2DA.

The interaction and binding energies and BSSE-corrected energies of the various ligands in the case of model A at the HF/6-31G** and B3LYP/6-31G** levels are presented in Table 3. Here, we define the binding energy (BE) as the sum of the interaction energy (INT) and relaxation energy (RLX), as follows.

$$\mathrm{BE} = \mathrm{INT} + \mathrm{RLX} \quad (1)$$

In order to assess the interaction of the hydroxy fatty acids with the estrogen receptor, we compared their interaction and binding energies to those of the original ligand GEN. The interaction energy of 9HNA is as large as that of GEN. For 10HDA, 10H2DA, and 10,10H2DA, the interaction energies are smaller by 17–25 kJ mol^{-1}. Although the interaction energy of 9,10,10H2DA is much larger than that of GEN, it becomes smaller when the relaxation energy is taken into account, as mentioned below. The tendency in the interaction energy was not changed by the BSSE correction.

The number of H-bonds is reflected in the sequence in the interaction energy for both saturated and unsaturated hydroxy fatty acids as follows, 10H2DA > 8H2DA > 9H2DA > 7H2DA and 9HNA > 10HNA > 8HOA. However, these tendencies disappear in the binding energies, where the contribu-

Table 3. Interaction and Binding Energies (kJ mol^{-1}) of the Various Ligands in Model A at the HF/6-31G** and B3LYP/6-31G** (in Parentheses) Levels

Ligand	INT	INT+ BSSE corr.	BE	BE+BSSE corr.
GEN	172.8 (206.7)	144.8 (161.5)	97.1 (125.1)	69.0 (79.9)
10H2DA	149.4 (186.6)	119.2 (137.7)	62.3 (90.8)	32.2 (41.8)
9H2DA	84.9 (101.3)	67.4 (72.4)	72.8 (87.0)	55.2 (57.7)
8H2DA	115.9 (138.5)	92.9 (101.3)	68.6 (87.4)	46.0 (49.8)
7H2DA	61.9 (73.2)	48.5 (50.6)	51.0 (63.6)	37.2 (41.0)
10HDA	157.7 (195.4)	128.4 (147.3)	64.4 (92.0)	35.1 (43.9)
9HNA	172.8 (210.0)	143.1 (161.1)	82.0 (113.0)	52.3 (64.0)
8HOA	79.9 (91.6)	65.3 (69.0)	66.5 (80.3)	51.9 (57.7)
10,10H2DA	160.2 (197.9)	128.9 (148.1)	63.6 (95.0)	31.8 (43.5)
9,10,10H2DA	252.3 (295.0)	210.0 (227.2)	94.1 (117.2)	52.3 (49.4)

Table 4. Distances of the H-Bonds of the Various Ligands with the Surrounding Amino Acid Residues and Bound Water and the Selected Dihedral Angles of the Ligands in the Optimized Structures of Model B at the ONIOM(HF/6-31G*:PM3) Level

Ligand	Distance of the H-bonds/Å				Dihedral angle/degree	
	Glu305	Arg346	Bound water	His475	∠2–3–4–5	∠10–9–8–7
GEN	1.597	1.935		1.898	46.2	
10H2DA	1.758	2.454/2.472		1.904	−90.5	−179.7
9H2DA				1.887	−89.1	−177.6
8H2DA				1.889	−91.2	179.8
7H2DA				1.891	−89.0	179.7
10HDA	1.756	2.443/2.455		1.922	−58.8	179.6
9HNA	1.759	1.980/2.955		1.916	−60.8	176.7
8HOA	1.927			1.898	−81.4	−173.7
10,10H2DA	1.872/1.887	2.013		1.904	−86.0	−147.8
9,10,10H2DA	1.734	2.024/2.554/2.648	1.854	1.897	−90.6	−177.7

tion of relaxation energy is significant. Here, it should be noted that the BSSE-corrected binding energies of 9HNA, 8HOA, and 9H2DA are not so small compared to that of GEN.

ONIOM Calculations for Model B. In order to examine the environmental effects on the H-bonds of the ligands with Glu305, Arg346, His475, and the bound water, we adopted model B with ten additional amino acid residues that surround the ligand and form the shape of the pocket of the active site. We optimized the structures and calculated the binding energies for model B by the ONIOM method and compared these to those for model A to clarify the environmental effects.

The optimized geometric parameters at the ONIOM(HF/6-31G*:PM3) level for the various ligands are listed in Table 4. We do not find any significant difference in the dihedral angle ∠2–3–4–5 and the H-bond distances between models A and B for GEN. However, it should be noted that the steric restriction inside the pocket does not allow GEN to form the H-bond with bound water found in model A. By the same reason, the –OH group cannot form any H-bond not only for 7H2DA but also for 9H2DA and 8H2DA. Although the –OH oxygen of 10H2DA forms two H-bonds with two NH hydrogen of Arg346, both distances are elongated by about 0.7 Å.

As shown in Figure S4, the carbon chain is arranged to straight form except the –CH=CH–COOH part for all unsaturated hydroxy fatty acids. This change in the carbon chain is reflected especially in the dihedral angle ∠10–9–8–7 of almost 180° for 10H2DA, 9H2DA, 8H2DA, and 7H2DA. On the other hand, the dihedral angle ∠2–3–4–5 is decreased to about −90°, because the relaxation of His475 is restricted by a steric contact with the other neighboring amino acid residues. It should be noted that the dihedral angle ∠2–3–4–5 is −89.0° even for 7H2DA (It is −0.6° in model A. See, the previous section).

For the saturated hydroxy fatty acids of 9HNA, the H-bond of the –OH group with the bound water is lost, and instead, the –OH oxygen forms two H-bonds with the two NH hydrogens of Arg346. The C2–C3–C4–C5 chain of all the saturated hydroxy fatty acids, 10HDA, 9HNA, and 8HOA, takes a gauche conformation as shown by the dihedral angle ∠2–3–4–5 of about 60–80° due to steric restriction, which is different from the case of model A. On the other hand, the dihedral angle ∠10–9–8–7 of the saturated hydroxy fatty acids is not deviated much from 180°.

Table 5. Interaction and Binding Energies (kJ mol^{-1}) of the Various Ligands in Model B at the ONIOM(HF/6-31G**:PM3) and ONIOM(B3LYP/6-31G**:PM3) (in Parentheses) Levels[a)]

Ligand	INT	INT(inner)	INT(inner) +BSSE corr.	INT(outer)	Ratio of INT(inner)/%	BE	BE+BSSE corr.
GEN	201.3 (231.4)	166.1 (196.2)	141.0 (156.1)	35.1 (35.1)	345.6 (354.8)	119.2 (143.1)	94.1 (102.9)
10H2DA	175.3 (205.0)	106.7 (136.4)	80.3 (95.0)	68.6 (68.6)	254.4 (278.2)	113.4 (136.4)	87.0 (95.0)
9H2DA	102.9 (119.2)	38.5 (54.8)	22.2 (30.1)	64.4 (64.4)	156.5 (191.6)	55.6 (77.0)	39.3 (52.3)
8H2DA	110.9 (127.6)	38.9 (55.2)	22.6 (31.0)	72.0 (72.4)	146.4 (181.6)	73.2 (94.1)	56.9 (69.5)
7H2DA	101.7 (118.4)	36.4 (53.1)	20.5 (28.9)	65.3 (65.7)	149.8 (187.0)	63.6 (84.5)	47.3 (60.7)
10HDA	189.5 (219.2)	111.7 (141.4)	84.9 (99.2)	77.4 (77.4)	247.3 (270.3)	125.5 (146.0)	98.3 (103.8)
9HNA	203.3 (232.2)	143.5 (172.4)	120.0 (132.6)	59.8 (59.8)	295.4 (310.5)	156.9 (178.2)	133.1 (138.9)
8HOA	134.3 (149.0)	81.2 (95.4)	67.4 (73.6)	53.1 (53.1)	252.7 (268.6)	122.6 (139.3)	108.8 (117.2)
10,10H2DA	231.4 (265.3)	178.2 (212.5)	145.2 (160.2)	52.7 (52.7)	322.6 (335.1)	139.7 (166.9)	106.3 (114.6)
9,10,10H2DA	233.9 (276.1)	161.9 (203.8)	129.7 (152.7)	72.0 (72.0)	289.5 (309.2)	114.6 (147.7)	82.8 (96.7)

a) INT(inner) and INT(outer) mean the interaction energy of the ligand with the amino acid residues and the bound water in the inner part and the interaction energy of the ligand with the amino acid residues in the outer part, respectively. INT = INT(inner) + INT(outer). The BSSE correction is taken into account only for INT(inner).

Also for 10,10H2DA, the H-bond of the –OH group with the bound water is lost. However, the dihedral angle ∠10–9–8–7 of −147.8° is still small due to the strong interaction between two –OH groups at the C-10 position and the two oxygens of the –COO$^-$ of Glu305. For both 10,10H2DA and 9,10,10H2DA, the dihedral angle ∠2–3–4–5 decreases to about −90° due to the same steric restriction mentioned above.

The binding and interaction energies and their BSSE-corrected energies for the various ligands at the ONIOM(HF/6-31G**:PM3) and ONIOM(B3LYP/6-31G**:PM3) levels are listed in Table 5. For GEN, the interaction energy increases by 25–29 kJ mol^{-1} in model B. The ratio of the interaction energy of the inner part against the interaction energy of the entire system is relatively large compared to those for the fatty acids. When the relaxation energy is taken into account, the interaction energy is reduced by about 84 kJ mol^{-1} as shown by the binding energy, which is similar to the case of model A.

Although the interaction energy of the entire system for 10H2DA is similar to that for GEN, the interaction energy of the inner part is smaller and the interaction energy of the outer part is larger for10H2DA than that for GEN. The binding and BSSE-corrected binding energies for 10H2DA are also similar to those for GEN. For 9H2DA, 8H2DA, and 7H2DA, the binding energy as well as interaction energy is small due to the small interaction energy of the inner part that loses the H-bond for the –OH group. The BSSE-corrected binding energies for the saturated hydroxy fatty acids of 10HDA, 9HNA, and 8HOA are larger than that for GEN. In particular, it is larger by 38 kJ mol^{-1} in the case of 9HNA. This fact would be attributed to the difference in the interaction energy of the outer part and in the relaxation energy between 9HNA and GEN. The relaxation energy is smaller by 33–38 kJ mol^{-1} for 9HNA than for GEN. This means that 9HNA fits the pocket better compared to GEN. The interaction energy of the outer part is about two times larger for 9HNA than for GEN, while the interaction energy of the inner part for 9HNA is as large as that for GEN.

As we expected, the interaction energies for 10,10H2DA and 9,10,10H2DA are larger by 29–42 kJ mol^{-1} than that for GEN due to some additional H-bonds. However, when the relaxation energies are taken into account, these interaction energies are much reduced and then the binding energies for both 10,10H2DA and 9,10,10H2DA become nearly the same as that for GEN.

MD Simulations for Model B. We performed MD simulations at 300 K for model B in order to examine the effects of the motion of the ligands inside the pocket on the H-bonds qualitatively. Besides the original ligand GEN, we selected 10H2DA and 9HNA from each group of the unsaturated and saturated hydroxy fatty acids, since both exhibited the largest binding energy in each group (see Table 5). Before running the MD simulations, we re-optimized the structure of model B for GEN, 10H2DA, and 9HNA with the MM3 force field, and confirmed that the H-bonds formed inside the pocket between these ligands and the amino acid residues at the ONIOM(HF/6-31G*:PM3) level are reproduced. When the temperature was increased to 300 K, the thermal motion of the entire system affected the H-bonds of the ligands with the amino acid residues, Glu305, Arg346, and His475 and the bound water.

We examined probabilities of the formation of H-bonds of the ligands with Glu305, Arg346, His475, and the bound water in the MD simulations. The probabilities of the formation of H-bond between the –OH hydrogen of the ligands and the amino acid residues or the bound water are presented in Table 6. In the case of GEN, one of the –OH hydrogens stays not far from the –COO$^-$ group of Glu305. Nevertheless, the –OH hydrogen hardly comes close to either oxygen of the –COO$^-$ group. Therefore, the –COO$^-$ group of Glu305 forms a H-bond network with the N–H of Arg346 and the bound water. The –OH hydrogen forms the H-bond mainly with the CO oxygen of the main chain of Lue339, the average and standard deviation of this H-bond distance being 2.217 and 0.342 Å, respectively. This position of –OH hydrogen would be at a local minimum lying higher in energy. This –OH group also forms a H-bond with the bound water oxygen with a relatively high

Table 6. Probabilities (%) of the Formation of the H-Bond between the –OH Hydrogen of the Ligands and the Amino Acid Residues or the Bound Water with the Distances of less than 3.0 and 2.5 Å in the Molecular Dynamics Simulations for Mode B at 300 K

Ligand	Glu305(O1/O2, side chain)		Bound water(O)		Leu339(CO, main chain)	
	3.0 Å	2.5 Å	3.0 Å	2.5 Å	3.0 Å	2.5 Å
GEN	1.7/1.3	0.6/0.1	45.4	6.7	95.7	86.8
10H2DA	86.7/74.4	79.4/65.1	5.0	0.1	0.0	0.0
9HNA	77.1/96.5	68.1/89.1	10.1	0.2	0.0	0.0

Table 7. Probabilities (%) of the Formation of the H-Bond between the –OH Oxygen of the Ligands and the Amino Acid Residues or the Bound Water with the Distances of less than 3.0 and 2.5 Å in the Molecular Dynamics Simulations for Mode B at 300 K

Ligand	Arg346(H1/H2, side chain)		Arg346(H3/H4, side chain)		Bound water(H1/H2)	
	3.0 Å	2.5 Å	3.0 Å	2.5 Å	3.0 Å	2.5 Å
GEN	0.0/0.0	0.0/0.0	47.5/39.6	26.0/19.6	7.0/7.8	0.3/0.7
10H2DA	10.7/3.4	2.7/0.9	33.2/13.3	37.0/18.9	11.7/9.1	4.3/0.9
9HNA	4.1/9.2	2.2/3.5	49.3/41.0	23.6/16.7	18.3/18.6	6.0/4.0

Table 8. Probabilities (%) of the Formation of the H-Bond between the –COOH Hydrogen or –OH Hydrogen of the Ligands and the Amino Acid Residues with the Distances of Less than 3.0 and 2.5 Å in the Molecular Dynamics Simulations for Mode B at 300 K

Ligand	His475(N, side chain)		Leu476(NH, main chain)		Gly472(CO, main chain)		Leu298(CO, main chain)	
	3.0 Å	2.5 Å	3.0 Å	2.5 Å	3.0 Å	2.5 Å	3.0 Å	2.5 Å
GEN	93.5	73.2	1.5	0.0	0.2	0.0	0.0	0.0
10H2DA	15.9	6.0	0.3	0.0	0.2	0.0	0.0	0.0
9HNA	48.7	28.0	5.2	0.0	22.8	18.1	1.3	0.7

Table 9. Probabilities (%) of the Conformation of the Local Chains Consisting of Four Carbons of the Ligands, 10H2DA and 9HNA, in the Molecular Dynamics Simulations for Model B at 300 K[a)]

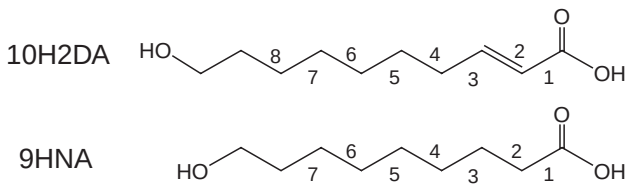

Ligand	Axis 1[b)]		Axis 2		Axis 3[c)]		Axis 4		Axis 5		Axis 6		Axis 7		Axis 8	
	trans	cis	trans	gauche	skew /trans	cis /gauche	trans	gauche	trans	gauche	trans	gauche	trans	gauche	trans	gauche
10H2DA	100.0	0.0			81.4	8.6	100.0	0.0	77.4	21.0	44.4	53.6	93.7	4.9	65.0	32.6
9HNA	65.3	8.6	80.9	17.2	27.4	71.2	96.1	2.9	96.1	2.8	96.1	2.7	46.2	52.1		

a) For the axes 2–8 of the single bond, the dihedral angle of more than 140° was counted as trans, and the dihedral angle of less than 100° was counted as gauche. b) "Trans" means that the –OH group is trans to the carbon. The dihedral angle of more than 140° was counted as trans, and the dihedral angle of less than 40° was counted as cis. c) For the axis 3 of 10H2DA, the dihedral angle of more than 80° was counted as skew, and the dihedral angle of less than 40° was counted as cis.

probability. On the other hand, the other –OH hydrogen maintains a H-bond with His475 as shown in Table 8 with an average distance of 2.412 Å and a standard deviation of 0.450 Å. The vibration of this H-bond, OH···N(His475) (see Figure 1), seems to cause a small rotation of the entire GEN and moves the position of the other –OH group slightly downward.

In contrast, for 10H2DA, the –OH hydrogen strongly interacts with the $-COO^-$ oxygen of Glu305 and the –OH oxygen interacts with the NH hydrogen of Arg346 as shown by the high probabilities of their H-bond formation presented in Tables 6 and 7. Table 6 shows the –OH group a little far from the bound water. On the other hand, the –COOH group stays far from His475 and sometimes comes close to His475, which is shown by the low probability of H-bond formation (Table 8). The –COOH group does not have any interaction with other neighboring amino acid residues, even when the –COOH group goes away from His475.

We also examined the change in the conformation of the local chain consisting of four carbons during the simulation. As presented in Table 9, for 10H2DA, the local chains with

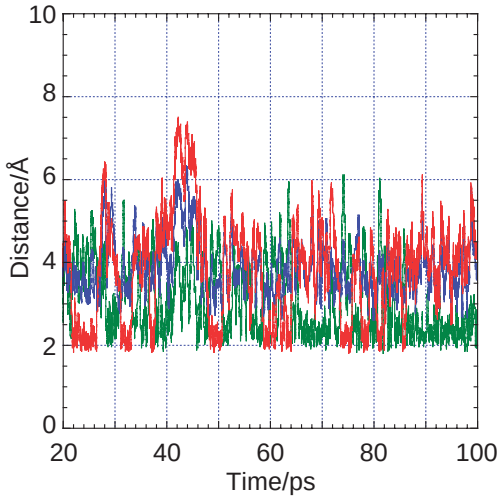

Figure 3. Changes in the distances of the selected H-bonds in the MD simulation of model B at 300 K for 9-hydroxynonanoic acid (9HNA). The color of the lines represents the distances as follows; green: the distance between the –COOH hydrogen and His475, blue: the distance between the –COOH hydrogen and the NH nitrogen of the main chain of Leu476, and red: the distance between the –COOH hydrogen and the CO oxygen of the main chain of Gly472.

the axes 5, 6, and 8, which are located far from the chain 1–2–3–4, take a gauche form with relatively high probability. On the other hand, the local chain with the axis 3 keeps a skew conformation. This rigid conformation of the 2–3–4–5 chain would reduce the flexibility in the motion of the –COOH terminal and prohibit the –COOH group from interacting with the surrounding amino acid residues as mentioned above.

9HNA as well as 10H2DA show strong interaction with Glu305 through the H-bond of the –OH group with the $–COO^-$ oxygen, as shown by the high probability of H-bond formation in Table 6. The –OH oxygen also forms H-bonds with the NH of Arg346 and the bound water hydrogen (Table 7). On the other hand, the –COOH hydrogen does not always interacts with His475, which is similar to the case of 10H2DA. However, in contrast to the case of 10H2DA, even if the –COOH hydrogen goes away from His475, the –COOH hydrogen interacts with other neighboring amino acid residues, i.e., the CO oxygen of the main chain of Gly472, the NH nitrogen of the main chain of Leu476, and the CO oxygen of the main chain of Leu298, as shown by both Figure 3 and Table 8. It should be noted that besides the local chain with axis 7, the local chains with the axes 2 and 3, which are located on the right hand side of the skeletal formula, take a gauche conformation with a high probability (Table 9). In addition, the –COOH group rotates around the axis 1. This flexible motion of the carbon chain on the –COOH side for a saturated fatty acid 9HNA, which was not found for an unsaturated fatty acid 10H2DA, would be an advantage in the interaction with the active site of the estrogen receptor.

Conclusion

The pharmacological effects of royal jelly similar to those caused by the hormone estrogen are thought to appear as a result of important fatty acids present in royal jelly acting as an agonist towards an estrogen receptor inside the human body. However, any direct evidence suggesting the interaction of the fatty acids with the estrogen receptor has not been reported yet. In this study, we therefore examined the interaction of a set of hydroxy fatty acids with a model pocket of the active site of the human estrogen receptor β using quantum mechanical (QM), ONIOM, and molecular dynamics (MD) methods.

Both QM and ONIOM methods showed that both saturated and unsaturated hydroxy fatty acids can fit the pocket and interact with the active site of the estrogen receptor. The terminal –OH and –COOH groups of the fatty acids interact with three essential amino acid residues, Glu305, Arg346, and His475, and the bound water of the active site through H-bonds. The other surrounding amino acid residues significantly affect the H-bonds of the ligand with these three amino acid residues and the bound water. The sterically restricted space of the pocket controls the interaction of the ligands. The binding energy of 84–126 kJ mol^{-1} similar to that for the original ligand genistein (GEN) was calculated for the unsaturated hydroxy fatty acids, (*E*)-10-hydroxy-2-decenoic acid (10H2DA), (*E*)-10,10-dihydroxy-2-decenoic acid (10,10H2DA), and (*E*)-9,10,10-trihydroxy-2-decenoic acid (9,10,10H2DA), and the saturated hydroxy fatty acids, 10-hydroxydecanoic acid (10HDA), 9-hydroxynonanoic acid (9HNA), and 8-hydroxyoctanoic acid (8HOA). The contribution of the electrostatic interaction with the amino acid residues environment excluding Glu305, Arg346, and His475 to the interaction energy was about 20–30% for these fatty acids. The MD simulations also gave additional interesting information concerning the thermal motion of the ligand inside the pocket.

Thus, our calculations suggest that the fatty acids involved in royal jelly can interact with the human estrogen receptor. The calculated large binding energy for 9HNA, 10,10H2DA, and 9,10,10H2DA, which have not been detected from royal jelly so far, will stimulate the experimentalists to search for new ingredients in royal jelly and give important information for design of new ligands.

TM and MA were supported in part by grants from the Ministry of Education, Culture, Sports, Science and Technology of Japan.

Supporting Information

Figures S1–S6 presenting models A and B optimized with the ligands, genistein (GEN), (*E*)-10-hydroxy-2-decenoic acid (10H2DA), (*E*)-9-hydroxy-2-decenoic acid (9H2DA), (*E*)-8-hydroxy-2-decenoic acid (8H2DA), (*E*)-7-hydroxy-2-decenoic acid (7H2DA), 10-hydroxydecanoic acid (10HDA), 9-hydroxynonanoic acid (9HNA), 8-hydroxyoctanoic acid (8HOA), (*E*)-10,10-dihydroxy-2-decenoic acid (10,10H2DA), and (*E*)-9,10,10-trihydroxy-2-decenoic acid (9,10,10H2DA), at the HF/6-31G* and ONIOM-(HF/6-31G*:PM3) levels, Table S1 presenting the H-bond distances of the ligands, genistein (GEN), (*E*)-10-hydroxy-2-decenoic acid (10H2DA), and 9-hydroxynonanoic acid (9HNA), in the optimized structures of model B at the MM3 level, Table S2 presenting the interaction energies of the ligands, genistein (GEN), (*E*)-10-hydroxy-2-decenoic acid (10H2DA), and 9-hydroxynonanoic acid (9HNA), in model B at the MM3 level, and listings

giving the Cartesian coordinates of these optimized structures. This material is available free of charge on the Web at http://www.csj.jp/journals/bcsj/.

References

1 M. H. Haydak, *Annu. Rev. Entomol.* **1970**, *15*, 143.

2 N. G. Patel, M. H. Haydak, T. A. Gochnauer, *Nature* **1960**, *186*, 633.

3 R. F. A. Moritz, E. E. Southwick, *Bees as Superorganism. An Evolutionary Reality*, Springer Verlag, Berlin, Heidelberg, **1992**.

4 S. Inoue, S. Koya-Miyata, S. Ushio, K. Iwaki, M. Ikeda, M. Kurimoto, *Exp. Gerontol.* **2003**, *38*, 965.

5 M. Kamakura, N. Mitani, T. Fukuda, M. J. Fukushima, *J. Nutr. Sci. Vitaminol.* **2001**, *47*, 394.

6 I. Okamoto, Y. Taniguchi, T. Kunikita, K. Kohno, K. Iwaki, M. Ikeda, M. Kurimoto, *Life Sci.* **2003**, *73*, 2029.

7 C. Bincoletto, S. Eberlin, C. A. Figueiredo, M. B. Luengo, M. L. Queiroz, *Int. Immunopharmacol.* **2005**, *5*, 679.

8 J. Vittek, *Experientia* **1995**, *51*, 927.

9 T. Matsui, A. Yukiyoshi, S. Doi, H. Sugimoto, H. Yamada, K. Matsumoto, *J. Nutr. Biochem.* **2002**, *13*, 80.

10 A. Fujii, S. Kobayashi, N. Kuboyama, Y. Furukawa, Y. Kaneko, S. Ishihama, H. Yamamoto, T. Tamura, *Jpn. J. Pharmacol.* **1990**, *53*, 331.

11 T. Takenaka, *Honeybee Sci.* **1982**, *3*, 69.

12 S. Fujiwara, J. Imai, M. Fujiwara, T. Yaeshima, T. Kawashima, K. Kobayashi, *J. Biol. Chem.* **1990**, *265*, 11333.

13 N. Noda, K. Umebayashi, T. Nakatani, K. Miyahara, K. Ishiyama, *Lipids* **2005**, *40*, 833.

14 G. F. Townsend, J. F. Morgan, B. Hazlett, *Nature* **1959**, *183*, 1270.

15 S. Pollet, C. Bottex-Gauthier, M. Li, P. Potier, A. Favier, D. Vidal, *Immunopharmacol. Immunotoxicol.* **2002**, *24*, 527.

16 S. Koya-Miyata, I. Okamoto, S. Ushio, K. Iwaki, M. Ikeda, M. Kurimoto, *Biosci., Biotechnol., Biochem.* **2004**, *68*, 767.

17 W. L. Winston, K. N. Slessor, M. J. Smirle, A. A. Kandil, *J. Chem. Ecol.* **1982**, *8*, 1283.

18 K.-M. Suzuki, Y. Isohama, H. Maruyama, Y. Yamada, Y. Narita, S. Ohta, Y. Araki, T. Miyata, S. Mishima, *eCAM* **2008**, *5*, 295.

19 D. J. Rickard, D. G. Monroe, T. J. Ruesink, S. Khosla, B. L. Riggs, T. C. Spelsberg, *J. Cell. Biochem.* **2003**, *89*, 633.

20 J. Wang, F. Shang, L. Liu, S. Wang, J. Wang, Q. Mei, *Indian J. Pharmacol.* **2007**, *39*, 103.

21 A. C. W. Pike, A. M. Brzozowski, R. E. Hubbard, T. Bonn, A. G. Thorsell, O. Engstrom, J. Ljunggren, J. A. Gustafsson, M. Carlquist, *EMBO J.* **1999**, *18*, 4608.

22 M. J. Frisch, G. W. Trucks, H. B. Schlegel, G. E. Scuseria, M. A. Robb, J. R. Cheeseman, J. A. Montgomery, Jr., T. Vreven, K. N. Kudin, J. C. Burant, J. M. Millam, S. S. Iyengar, J. Tomasi, V. Barone, B. Mennucci, M. Cossi, G. Scalmani, N. Rega, G. A. Petersson, H. Nakatsuji, M. Hada, M. Ehara, K. Toyota, R. Fukuda, J. Hasegawa, M. Ishida, T. Nakajima, Y. Honda, O. Kitao, H. Nakai, M. Klene, X. Li, J. E. Knox, H. P. Hratchian, J. B. Cross, V. Bakken, C. Adamo, J. Jaramillo, R. Gomperts, R. E. Stratmann, O. Yazyev, A. J. Austin, R. Cammi, C. Pomelli, J. W. Ochterski, P. Y. Ayala, K. Morokuma, G. A. Voth, P. Salvador, J. J. Dannenberg, V. G. Zakrzewski, S. Dapprich, A. D. Daniels, M. C. Strain, O. Farkas, D. K. Malick, A. D. Rabuck, K. Raghavachari, J. B. Foresman, J. V. Ortiz, Q. Cui, A. G. Baboul, S. Clifford, J. Cioslowski, B. B. Stefanov, G. Liu, A. Liashenko, P. Piskorz, I. Komaromi, R. L. Martin, D. J. Fox, T. Keith, M. A. Al-Laham, C. Y. Peng, A. Nanayakkara, M. Challacombe, P. M. W. Gill, B. Johnson, W. Chen, M. W. Wong, C. Gonzalez, J. A. Pople, *Gaussian 03, Revision C.02*, Gaussian, Inc., Wallingford CT, **2004**.

23 S. Simon, M. Duran, J. J. Dannenberg, *J. Chem. Phys.* **1996**, *105*, 11024.

24 S. F. Boys, F. Bernardi, *Mol. Phys.* **1970**, *19*, 553.

25 F. Maseras, K. Morokuma, *J. Comput. Chem.* **1995**, *16*, 1170.

26 T. Matsubara, S. Sieber, K. Morokuma, *Int. J. Quantum Chem.* **1996**, *60*, 1101.

27 T. Matsubara, F. Maseras, N. Koga, K. Morokuma, *J. Phys. Chem.* **1996**, *100*, 2573.

28 M. Svensson, S. Humbel, R. D. J. Froese, T. Matsubara, S. Sieber, K. Morokuma, *J. Phys. Chem.* **1996**, *100*, 19357.

29 S. Dapprich, I. Komáromi, K. S. Byun, K. Morokuma, M. J. Frisch, *THEOCHEM* **1999**, *461–462*, 1.

30 T. Vreven, K. Morokuma, *J. Comput. Chem.* **2000**, *21*, 1419.

31 K. Morokuma, *Bull. Korean Chem. Soc.* **2003**, *24*, 797.

32 J. W. Ponder, *TINKER, Software Tools for Molecular Design*, *Version 4.2*, Washington Univ., St. Louis, **2004**.

33 N. L. Allinger, Y. H. Yuh, J.-H. Lii, *J. Am. Chem. Soc.* **1989**, *111*, 8551.

34 J.-H. Lii, N. L. Allinger, *J. Am. Chem. Soc.* **1989**, *111*, 8566.

35 J.-H. Lii, N. L. Allinger, *J. Am. Chem. Soc.* **1989**, *111*, 8576.

36 J.-H. Lii, N. L. Allinger, *J. Phys. Org. Chem.* **1994**, *7*, 591.

37 J.-H. Lii, N. L. Allinger, *J. Comput. Chem.* **1998**, *19*, 1001.

38 D. Beeman, *J. Comput. Phys.* **1976**, *20*, 130.

39 H. J. C. Berendsen, J. P. M. Postma, W. F. van Gunsteren, A. DiNola, J. R. Haak, *J. Chem. Phys.* **1984**, *81*, 3684.

40 A. Karpfen, C. H. Choi, M. Kertesz, *J. Phys. Chem. A* **1997**, *101*, 7426.

41 M. A. Murcko, H. Castejon, K. B. Wiberg, *J. Phys. Chem.* **1996**, *100*, 16162.